Synthesis and in-depth characterization of reactive, uniform, crosslinked microparticles based on free radical copolymerization of 4-vinylbenzyl azide

Journal:	*Polymer Chemistry*
Manuscript ID	PY-ART-11-2015-001848.R1
Article Type:	Paper
Date Submitted by the Author:	15-Dec-2015

Complete List of Authors:	Albuszis, Marco; University of Hamburg, Technical and Macromolecular Chemistry Roth, Peter; Curtin University, Nanochemistry Research Institute Exnowitz, Franziska; University of Hamburg, Technical and Macromolecular Chemistry Wong, Doris; University of Hamburg, Technical and Macromolecular Chemistry Pauer, Werner; University of Hamburg, Technical and Macromolecular Chemistry Moritz, Hans-Ulrich; University of Hamburg, Technical and Macromolecular Chemistry

Synthesis and in-depth characterization of reactive, uniform, crosslinked microparticles based on free radical copolymerization of 4-vinylbenzyl azide

Marco Albuszis,[†] Peter J. Roth,[‡,*] Franziska Exnowitz,[†] Doris Locsin Wong,[†] Werner Pauer,[†,*] and Hans-Ulrich Moritz[†,*]

[†] Institute for Technical and Macromolecular Chemistry, University of Hamburg, Bundesstraße 45, 20146 Hamburg, Germany

[‡] Nanochemistry Research Institute and Department of Chemistry, Curtin University, Bentley, Perth WA 6102, Australia

Corresponding Author Email Addresses: P. J. Roth (peter.roth@curtin.edu.au), W. Pauer (pauer@chemie.uni-hamburg.de), H.-U. Moritz (moritzhu@chemie.uni-hamburg.de)

Keywords microparticles, tunable porosity, azide-functional microbeads, azide–alkyne click chemistry, seed-swelling polymerization, 4-vinylbenzyl azide

Abstract. The introduction of functional groups into microparticles is commonly accomplished through, at times, low-yielding post-synthesis modification. In this detailed study, the introduction of azide functionality into uniform, crosslinked, macroporous microparticles through direct copolymerization of styrene, divinylbenzene (DVB), and 4-vinylbenzyl azide (VBA) in varying ratios inside swollen polystyrene seed (template) particles is investigated. Formulations contained up to 40 wt-% of VBA in the monomer mixture. Resulting microspheres were characterised by SEM, porosimetry, FT-IR spectroscopy, and CHN elemental analysis. Uniform spherical particles with diameters ranging from 7.3 to 10.8 μm with diameter dispersities typically below 1.01 and with tuneable azide loadings from 0.11 to 1.17 mmol/g were obtained. Interestingly, severe effects of VBA addition on porosity, surface smoothness, and particle shape were observed. Specific surface areas and cumulative pore volumes increased with the amount of DVB in feed, decreased with increasing VBA feed ratio, and increased drastically for the use of azide-functional template particles with measured cumulative pore volumes reaching up to 0.60 cm^3/g. With increasing VBA feed, formation of smaller, secondary particles was observed and attributed to an incomplete swelling of VBA into seed particles, which is discussed as a main reason for lower-than-expected azide contents in product particles. For high VBA feed ratios (> 25 wt%), dented, hollow, or hollow collapsed azide-functional particles were found, presumably due to immiscibility of the growing azide-functional copolymer with the polystyrene seeds. Finally, successful click-modification is demonstrated with phenylacetylene and an alkyne-functional Rhodamine B dye allowing for mapping of functionalization density through confocal fluorescence microscopy.

Introduction

Serving widespread applications from chromatographic packing materials[1-4] to carriers for enzymes and catalysts,[5-7] crosslinked polymer microspheres have been attracting attention for several decades.[8] A range of synthetic routes toward well-defined, uniform microspheres has been developed to cater for very diverse use-oriented requirements including scale-up and industrial implementation. To date, precipitation polymerization and polymerization in suspension, water-based emulsion, and dispersion cover the vast majority of synthetic approaches.[9-13] More recently, microfluidic setups have been investigated for the preparation of well-defined polymer particles, typically in the size range of several hundreds of micrometres.[9, 14, 15]

Apart from particle diameter, important characteristics in determining applicability include, among others, surface texture, presence and degree of porosity, specific surface area, specific pore volume, mechanical properties, and chemical surface functionality. A key multi-step route toward micrometer-sized particles with tuneable size and porosity was developed by Ugelstad in the late 70s.[16-19] In this method, sub-micrometer-sized seed particles, typically consisting of linear polystyrene, are prepared through precipitation or emulsion polymerization. In a second step, these seed particles are dispersed in an aqueous solution and are swollen with a mixture of monomer, crosslinker, plasticizer, initiator and organic solvent as porogen. Upon heating in a third step, crosslinked polymer is formed inside the seed particle templates, which, lacking covalent attachment to the new particle, can typically be removed through extraction. Since its first description several decades ago, this method has been optimized, almost exclusively, for copolymerization of styrene with divinylbenzene inside polystyrene seed particles,[9, 20] with a limited number of studies addressing copolymerizations involving vinylbenzyl chloride.[21-23] As a

result, an impressive amount of work in this field has demonstrated these seed–swelling polymerizations to be a highly versatile and efficient process in the preparation of uniform microspheres with tuneable sizes, shapes, degrees of crosslinking, pore geometries, and specific surface areas.[4, 24-28]

Chemical surface functionality of microparticles is crucial for many applications in which a defined specific or non-specific binding of relevant chemical or biological species to particles is required.[8] Arguably the most common synthetic strategy to introduce functional groups into poly(styrene-*co*-divinylbenzene) microparticles is through post-synthesis modification of residual pendant vinyl groups stemming from the divinylbenzene crosslinker. Indeed, a plethora of vinyl group chemistries has been applied to this end, including hydrobromination,[29-31] bromination,[31] epoxidation,[32] addition reactions[33] including radical thiol–ene modification,[34] and acetoxy mercuration,[35] all typically, however, with moderate conversions. Additionally, modification of phenyl side groups, for example through chloromethylation[36] and aminomethylation,[37] has been applied for the modification of polystyrene-based microparticles. A direct terpolymerization of styrene, divinylbenzene, and a functional comonomer, is, despite the obvious appeal of making the above modification reactions unnecessary, not a very common method.[38-40]

As a prototypical click reaction, the copper-catalysed alkyne–azide cycloaddition reaction (CuAAC) is an extremely versatile and robust modification reaction by virtue of its high functional group tolerance, high yields in organic solvents and water, regiospecificity, and absence of side products.[41-46] Several research groups have demonstrated the versatility of CuAAC on microparticles including solid and porous particles.[34, 47-49] For example, Frechet's group presented the template suspension polymerization of poly(glycidyl methacrylate-*co*-

ethylene dimethacrylate)-based beads and epoxide ring opening with sodium azide to prepare 'clickable' and porous microspheres.[50] For polystyrene-based systems, Karagöz et al. described the hydrobromination of residual vinyl groups in solid poly(divinylbenzene) particles followed by nucleophilic substitution of the bromide groups with sodium azide and click modification.[30] Using a similar synthetic approach, our group recently demonstrated the modification of vinyl groups into azide functionality on porous poly(styrene-*co*-divinylbenzene) microspheres.[29] Urbani et al.[40] performed a terpolymerization of styrene, divinylbenzene, and vinylbenzyl chloride that resulted in a gel, which was ground, and the resulting powder subjected to substitution with sodium azide[51] and click modification. Conversely, Evans et al. presented the successful click-modification of alkyne-functional emulsion-made microparticles with a fluorescent dye.[49]

Notably, all of these methods rely on one or more post-synthesis modification steps in order to introduce the desired azide functionality. Given the typically low conversions of such modification steps on (macroporous or solid) microspheres, a copolymerization employing an azide functional monomer such as 4-vinylbenzyl azide can be expected to result in higher functional group densities without the need of additional post-synthesis steps. Reports on the use of 4-vinylbenzyl azide for microparticle synthesis[52, 53] are, however, limited and have, to the best of our knowledge, not been applied to seed-swelling polymerization formulations which allow for tuning of particle porosity.

Herein, we present a first detailed study into the feasibility of incorporating 4-vinylbenzyl azide, as a versatile building block for subsequent click modification, into seed-swelling polymerization formulations. Four different seed particles, including two azide-functional samples, were swollen in aqueous solution with toluene as porogen, plasticiser, and mixtures of

styrene, divinylbenzene, and 4-vinylbenzyl azide in varying molar ratios, followed by polymerization of the mixtures inside the template particles and purification. Through systematic variation of feed ratios and in-depth characterisation of all resulting particles through SEM, FT-IR, elemental analysis, and porosimetry, we demonstrate that well-defined microparticles with a tuneable content of azide functionality are accessible. As expected, the maximum azide content achieved through this method was higher than the maximum azide loading achieved in a previous study of our group using post-synthesis modification. Interestingly, however, the incorporation of 4-vinylbenzyl azide was found to have dramatic effects on porosity (including specific surface areas and volumes) and particle shapes. The use of azide-functional seed particles as templates, while not contributing to the azide content of the purified crosslinked microparticles, is shown to drastically increase porosity. Formulations including high feed ratios of 4-vinylbenzyl azide and divinylbenzene are demonstrated to produce hollow azide-functional particles. Finally, successful click-modification of azide groups in 52–100% yield using phenylacetylene or an alkyne-functional Rhodamine B dye is described together with characterisation of the modification density through confocal fluorescence microscopy. This very detailed study is expected to contribute to the understanding of processes and material compatibility influences during the preparation of well-defined, porous and functional microparticles.

Experimental Section

Materials. Unless otherwise noted, chemicals were purchased from Sigma Aldrich, Merck Chemicals, or Acros Organics in analytical grade and were used without further purification. Styrene (S) was distilled in vacuum to remove inhibitors and impurities directly before use. 2,2'-Azobis-(2-isobutyronitrile) (AIBN) was recrystallized from methanol. Divinylbenzene (DVB) was of technical grade containing 60–65 wt% divinylbenzene monomers and predominantly 3/4-ethylvinylbenzene as impurity. 4-Vinylbenzyl chloride was of 90% technical grade and freshly distilled in vacuum directly before use.

4-Vinylbenzyl Azide (VBA). To a solution of 4-vinylbenzyl chloride (10.8 mL, 7.7 mmol) in DMF (150 mL) was added sodium azide (15 g, 23.1 mmol). The suspension was stirred for 48 h at room temperature before diluting with 300 mL water. The product was extracted with diethyl ether (3× 300 mL). The organic phase was washed with brine (3× 200 mL) and dried over $MgSO_4$ before evaporating the solvent in vacuum. The product (12.1 g, 7.6 mmol, 99 %) was obtained as an orange oil. ^{1}H-NMR (400 MHz, DMSO-d_6) δ/ppm = 7.45–7.42 (m, 2 H, Ar*H*), 7.30–7.27 (m, 2 H, Ar*H*), 6.73 (dd, 1 H, J = 17.4 Hz, J = 10.8 Hz, Ar–C*H*=CH_2), 5.77 (dd, 1 H, J = 17.4 Hz, J = 0.9 Hz, Ar–CH=CH_2), 5.29 (dd, 1 H, J = 10.8 Hz, J = 0.9 Hz, Ar–CH=CH_2), 4.32 (s, 2H, Ar–CH_2Cl).

Microsphere Synthesis. Reactive microspheres carrying azide functionality were prepared in a multistep procedure involving (i) dispersion polymerization synthesis of polystyrene seed particles, (ii) swelling of these seed particles with a plasticiser and porogen, and (iii) polymerization of monomer mixtures inside the seed particles.

Polystyrene (PS) Seed particles. PS seed particles were prepared in analogy to a previously reported procedure using a 1 L double walled glass reactor equipped with reflux condenser,

argon gas inlet, overhead stirrer (4-blade, 45°, stainless steel) connected through a gas tight magnetic coupling, attached to a recirculating heater.[10, 29] The synthesis of PS seed particles with a number-average diameter, D_n, of 3.60 μm, hereafter denoted seed A, is given as an example: Ethanol (360g) and polyvinylpyrrolidone (PVP-K30, M_n = 40 kg mol^{-1}, 12 g) and Aliquat 336 (4.8 g) were stirred in the reactor at 150 rpm, purged with argon for 30 minutes, and heated to 70 °C. A separately prepared and degassed mixture of styrene (120 g) and AIBN (1.2 g, 1 wt%) was added into the reactor and the polymerization was allowed to proceed for 24 h with stirring at 150 rpm. Microparticles were isolated by repeated washing–centrifugation cycles in hot water and ethanol followed by drying in vacuum. Seed B was prepared in analogy using more AIBN (2.4 g, 2 wt%).

Poly(styrene-*co*-4-vinylbenzyl azide), P(S-co-VBA), Seed Particles. Two more seed particles, denoted C and D were prepared as follows. Reactions were performed in 3-necked 250 ml double walled glass reactors connected to a thermostat and placed on a shaking plate without additional stirrers. Ethanol (135g), polyvinylpyrrolidone (PVP-K30, M_n = 40 kg mol^{-1}, 1.5 g), and Aliquat 336 (0.6 g) were mixed overnight and transferred into the reactor followed by purging with argon for 30 minutes while shaking at 150 rpm. The temperature was increased to 70 °C. In a separate flask a monomer mixture (15 g total) consisting of styrene (12 g or 14.25 g) and 4-vinylbenzyl azide (3 g (20 wt%) or 0.75 g (5 wt%)) and AIBN (0.3 g, 2 wt%) were mixed and purged with argon for 15 minutes before transferring the solution into the preheated reactor. The polymerization was run for 24 h with shaking at 150 rpm. The mixture was cooled to room temperature and the target seed particles were purified by repeated washing and centrifugation using ethanol (1×), hot water (1×), and ethanol (1×) for redispersing before drying in vacuum. ^{1}H NMR ($CDCl^3$) δ/ppm = 7.00, 6.50 (bm, Ph); 4.15 (–C$\underline{H}_2$N$_3$); 2.28–0.72 (bm, backbone).

Molar copolymer compositions were determined by comparison of the integrals of the benzylic protons (2 H) of VBA to those of the phenyl side chains (5 H for Sty, 4 H for VBA) and the backbone (3 H).

Seed swelling polymerization. Functional particles were prepared through modification of a previously published protocol.[54] Briefly, seed particles (1 g) were swollen in aqueous dodecylsulfate solution first with dibutylphthalate (2.5 g), then with a monomer mixture containing styrene, divinylbenzene, and 4-vinylbenzyl azide in varying amounts (6 g in total) as well as benzoylperoxide (0.25 g) as initiator and toluene (4 g) as porogen. Following addition of poly(vinylalcohol) as stabiliser and polymerization at 70°C for 24 h, the resulting (reactive) microspheres were characterized by FT-IR, nitrogen adsorption for determination of specific surface area, SEM, and elemental analysis for chemical composition. Results are presented and discussed in the text.

Rhodamine B Alkyne. A reactive alkyne handle was installed into Rhodamine B by esterification of its carboxylic acid group. Propargyl alcohol (0.60 mL) and Rhodamine B (3.52 g, 0,73 mmol) were dissolved in dry dichloromethane (60 mL). 4-(Dimethylamino)pyridine (DMAP, 0.84 g, 0,68 mmol) and *N*-(3-(dimethylamino)propyl)-*N'*-ethylcarbodiimide hydrochloride (EDC, 2.01 g, 10.5 mmol) were added and the reaction was stirred for 18 h at room temperature. The organic phase was washed with 1 N HCl (3×), 1 N $NaHCO_3$ (3×) and brine (1×), dried over $MgSO_4$ and concentrated by evaporating ~90 % of solvent. The red residue was diluted with THF (5 mL) and precipitated twice into diethyl ether (250 mL). The product was obtained by centrifugation as golden-purple solid (3.7 g, 95 %). ^{1}H-NMR (400 MHz, $CDCl_3$) δ/ppm = 8.27 (dd, 1H, *J* = 7.8 Hz, 1.2 Hz, COCC*H*), 7.79 (td, 2H, *J* = 7,5 Hz, 1.5 Hz, COCCCHC*H*), 7.70 (td, 2H, *J* = 7.6 Hz, 1.6 Hz, COCCHC*H*), 7.27 (dd, 1H, *J* = 7,5 Hz, 1.2 Hz,

COCCC*H*), 7.03 (s, 1H, NCCHC*H*), 6.99 (s, 1H), 6.86 (dd, 2H, *J* = 6.6 Hz, 2.4Hz, NCC*H*CH), 6.75 (d, 2H, *J* = 2.4 Hz, NCC*H*C), 4.57 (d, 2H, *J* = 2.4 Hz, OCH_2), 3.60 (q, 8H, *J* = 7.2 Hz, $CH_2CH_2CH_2$), 2.37 (t, 1H, *J* = 2.4 Hz, OCH_2C-C*H*), 1.27 (t, 12H, *J* = 7.2 Hz, CH_3). ^{13}C NMR (100 MHz, $CDCl_3$) δ/ppm = 164.2 (*C*=O), 158.2 (O(O)CC*C*-Ar), 157.7 (2× N*C*), 155.5 (2× O*C*), 133.7 (*C*CO(O)), 133.5, 131.5, 131.2, 130.5, 130.3 (5× Ar-H), 129.1 (*C*-Ar(COO)), 114.3 (NC*C*HCH), 113.5 (OC*C*), 96.3 (2× NC*C*HC), 76.5 (OCH_2*C*CH), 75.6 (OCH_2C*C*H), 52.9 (O*C*H_2), 46.2 (CH_3*C*H_2N), 12.7 (*C*H_3).

Click modification of azide functional P(S-DVB-VBA) microspheres. A general procedure is given: Azide-functional particles (100 mg) were mixed with DMF (5 mL), *N*,*N*,*N'*,*N'*-tetramethylethylendiamine (TMEDA), CuBr, and triethylamine (1 eq. each with regards to azide functionality), followed by purging with argon for 5 minutes. An alkyne functional reagent (phenylacetylene or Rhodamine B alkyne, 3-fold excess with regards to azide functionality) was added, the reaction sealed and stirred for 24 h at 50 °C before filtering and washing the particles with DMF, water, ethanol, and acetone (25 mL each), followed by drying in vacuum. Analytical data is presented and discussed in the text.

Characterization. Surface morphology and uniformity of particles were monitored by scanning electron microscopy (SEM, LEO1525). Particles were dispersed in ethanol with sonication and spread onto an aluminium specimen stub. After drying, samples were coated with a thin layer of carbon in vacuum. Energy dispersive X-ray spectroscopy (EDS) was performed using an EDAX TEAM EDS Analysis System coupled to the SEM instrument with an Octane Plus Si-Drift detector.

Particle diameters, d_n and diameter dispersities, $Đ_d$ were calculated by measuring at least 100 particles using Image J software. The coefficient of variation (*CV*), weight- (d_w) and number-

average (d_n) diameters were calculated using the following equations where n_i is the number of particles of diameter d_i:[55, 56]

$$d_w = \frac{\sum n_i d_i^4}{\sum n_i d_i^3}$$

$$d_n = \frac{\sum n_i d_i}{\sum n_i}$$

$$Đ_d = \frac{d_w}{d_n}$$

$$CV = \frac{[(\sum_{i=1}^{N}(d_i - d_n)^2)/(N-1)]^{1/2}}{d_n}\ x\ 100$$

Specific surface areas and cumulative pore volumes were determined by measuring nitrogen adsorption on a porosimeter (Thermo Scientific, Surfer) and calculated using Brunauer-Emmett-Teller theory.

Chemical transformations of microspheres were monitored by FT-IR spectroscopy on an ATR-FT-IR spectrometer Nicolet iS10 (Thermo Fisher Scientific).

Solution NMR spectra were measured on a Bruker Avance 400 spectrometer.

CHN elemental analysis was performed on EuroVector Euro EA or Elementar Vario EL III instruments. Combustion gases were detected by gas chromatography (Euro EA) or using a head conductivity detector (Vario EL III).

Weight average molecular weights (M_w) and molecular weight dispersities ($Đ_M$) of soluble polymer samples (seed particles) were determined by a size exclusion chromatography instrument equipped with three Agilent PLgel 10 μm mixed bed columns and a Schambeck SFD GmbH RI 2000 detector in THF as eluent. Reported molecular weights are polystyrene equivalent values.

Results and Discussion

Microsphere Synthesis

The synthesis of azide-functional microparticles followed a multistep protocol (Scheme 1): (i) dispersion polymerization of seed particles, (ii) swelling of seeds with plasticiser, porogen, a monomer mixture containing a crosslinker, and an initiator, and (iii) copolymerization inside the swollen seed latexes.[29] In this procedure, the seed particles act as a template for the production of much larger crosslinked particles and, consisting of non-crosslinked chains, are extracted from the final microspheres during purification. The incorporation of any microsphere functionality must therefore occur during the copolymerization inside the swollen seeds. To reiterate, the main objective of this work is to study the feasibility of incorporating azide functionality in this second step and the influence of 4-vinylbenzyl azide (VBA) comonomers on the size, morphology, and porosity of the resulting microparticles. To this end, VBA was prepared in excellent yield in one step from 4-vinylbenzyl chloride.

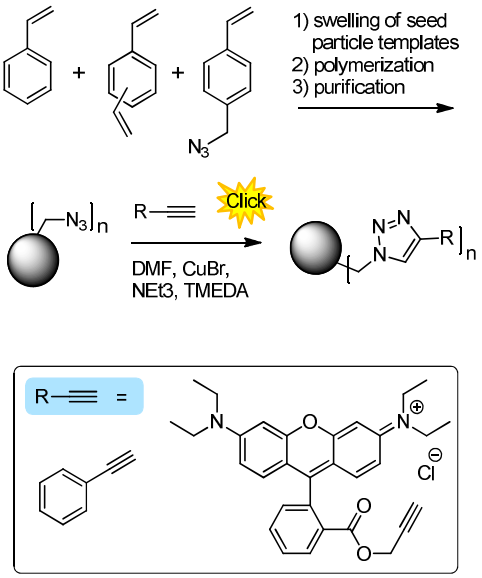

Scheme 1: Overview of microsphere synthesis with through copolymerization using 4-VBA in seed particle templates and functionalization via click-modification

Firstly, polystyrene (PS) and, in order to study the influence of the seed material, poly(styrene-*co*-4-vinylbenzyl azide) (P(S-*co*-VBA)) seed particles were prepared through dispersion polymerization of the respective monomers S and VBA in ethanol containing stabilisers from which compact, uniform, spherical seed particles precipitated. Seed particles were washed intensely with water and ethanol to remove stabilisers and characterised by SEM. Seed particles consisted of linear PS or P(S-*co*-VBA) chains and dissolved unimerically in THF, in which weight-average molecular weights were determined by SEC. Experimental details and size specifications of four seed particles, denoted A–D, are summarised in Table 1. For P(S-*co*-VBA) copolymers, monomer conversions were high and the resulting copolymers had molar compositions similar to the monomer feed ratios.

Table 1. Overview of Seed Particles Used in this Study

Seed Code	Description[a]	Feed			d_n[b] [μm]	$Đ_d$[c]	CV[d] [%]	M_w[e] [kg/mol]
		S:VBA [wt%]	S:VBA [mol%]	AIBN [wt%]				
A	PS	100:0	100:0	1	4.60	1.006	8.1	76
B	PS *(lower Mw)*	100:0	100:0	2	3.53	1.005	7.0	44
C	P($S_{0.97}$-*co*-$VBA_{0.03}$)	95:5	97:3	2	2.59	1.004	6.4	49
D	P($S_{0.87}$-*co*-$VBA_{0.13}$)	80:20	86:14	2	2.12	1.07	23.1	28

[a] indices give *molar* copolymer composition determined by ^{1}H NMR spectroscopy; [b] number-average particle diameter from SEM; [c] dispersity of the particle diameter; [d] coefficient of variation of the particle diameter; [e] polystyrene-equivalent weight-average molecular weight of dissolved polymer determined by SEC

In a second step, seed particles (typically 1 g) were dispersed in aqueous solution and swollen with dibutylphthalate (DBP), toluene, and a mixture (typically 6 g) of divinylbenzene (DVB, as

crosslinker), VBA and styrene (S), as well as benzoylperoxide (as initiator). Optical microscopy was used during the swelling process to monitor the disappearance of DBP droplets and swelling of the seed particles to a constant diameter. Following polymerization of the monomer mixture inside the swollen seed latexes the resulting crosslinked white to yellow microspheres (depending on VBA content) were purified by intensive Soxhlet extraction with water and THF, dried, and were characterised by FT-IR spectroscopy, SEM, BET nitrogen absorption, and CHN elemental analysis. Initially, the ratio of DVB:VBA:S was varied in three series using seed particles A. The first microsphere series, denoted LA, had a low content of 16 wt% of DVB crosslinker and 0–30 wt% of VBA in the monomer mixture. The second series, denoted MA, featured a medium, 50 wt%, DVB content and 0–40 wt% of VBA, while the last series, denoted HA, contained only DVB and VBA (0–35%), but no styrene. These feed ratios and analytical data of microspheres are summarised in Table 2, entries 1–27. Each series contained a non-functional reference sample made without VBA, i.e. samples LA0, MA0, HA0, that exhibited the expected spherical shape, uniform size distribution with diameter dispersities, $Đ_d$ as low as 1.007, and porous structure with high specific surface areas up to 341 m²/g and cumulative pore volumes up to 0.23 cm³/g. When higher amounts of toluene porogen was added, highly porous particles with specific surface areas of up to 747 m²/g and cumulative pore volumes of up to 1.14 cm³/g were produced, see supporting information.

Table 2. Overview of Microspheres

Entry	Code	Seeds[a]	Feed			SEM analysis			Nitrogen Adsorption		CHN analysis	
			DVB [wt%]	VBA [wt%]	S [wt%]	d_n[b] [µm]	$Đ_d$[c]	CV[d] [%]	S[e] [m^2/g]	V[f] [cm^3/g]	azide[g] [mmol/g]	N_1/N_0[h]
1	LA0	A	16	0	84	8.9	1.004	6.1	7.3	0.098	0	—
2	LA1	A	16	2.5	81.5	8.3	1.002	3.9	—	0.002	0.14	0.88
3	LA2	A	16	5	79	8.2	1.009	8.2	—	0.012	0.23	0.73
4	LA3	A	16	10	74	7.8	1.009	9.6	—	0.013	0.51	0.81
5	LA4	A	16	15	69	aggl.[i]	—	—	—	0.006	0.74	0.79
6	LA5	A	16	20	64	(7.4)	(1.005)	—	—	0.008	0.82	0.65
7	LA6	A	16	25	59	aggl.	—	—	—	0.004	0.89	0.57
8	LA7	A	16	30	54	aggl.	—	—	—	0.007	0.78	0.42
9	MA0	A	50	0	50	7.8	1.007	8.7	48.3	0.160	0	—
10	MA1	A	50	2.5	47.5	7.6	1.005	6.9	22.1	0.150	0.12	0.77
11	MA2	A	50	5	45	7.6	1.004	6.6	28.7	0.140	0.22	0.71
12	MA3	A	50	7.5	42.5	7.7	1.008	8.6	41.6	0.190	0.27	0.60
13	MA4	A	50	10	40	7.8	1.004	6.5	40.2	0.210	0.37	0.59
14	MA0	A	50	12.5	37.5	aggl.	—	—	—	0.012	0.43	0.54
15	MA6	A	50	15	35	9.8	1.002	5.3	—	0.007	0.44	0.46
16	MA7	A	50	17.5	32.5	(9.6)	—	—	5.7	0.022	0.48	0.44
17	MA8	A	50	20	30	(9.4)	(1.005)	(7.2)	—	0.006	0.64	0.51
18	MA9	A	50	30	20	(10.1)	(1.004)	(6.3)	—	—	0.80	0.42
19	MA10	A	50	40	10	coll.[j]	—	—	—	—	1.17	0.46
20	HA0	A	100	0	0	10.6	1.009	9.6	341	0.230	0	—
21	HA1	A	97.5	2.5	0	10.8	1.008	9.2	316	0.214	0.11	0.70
22	HA2	A	95	5	0	9.9	1.014	12.0	217	0.156	0.20	0.64
23	HA3	A	90	10	0	10.1	1.006	7.9	123	0.127	0.37	0.59
24	HA4	A	85	15	0	10.2	1.005	7.4	68.9	0.114	0.45	0.48
25	HA5	A	80	20	0	(7.1)	(1.013)	(11.4)	11.5	0.037	0.59	0.47
26	HA6	A	70	30	0	(8.9)	(1.005)	(7.2)	—	0.009	0.80	0.42
27	HA7	A	65	35	0	coll.	—	—	—	0.020	0.98	0.44
28	HB1	B	95	5	0	8.3	1.019	14.1	64.9	0.208	0.16	0.50
29	HB2	B	80	20	0	(7.3)	(1.014)	(12.4)	79.8	0.233	0.56	0.45
30	HC1	C	95	5	0	(9.0)[k]	(1.00029)[k]	(1.7)[k]	200	0.490	0.19	0.61
31	HC2	C	80	20	0	(8.0)[k]	(1.00027)[k]	(1.7)[k]	85.0	0.320	0.60	0.48
32	HD1	D	95	5	0	(8.7)[k]	(1.00026)[k]	(1.7)[k]	96.0	0.600	0.23	0.72
33	HD2	D	80	20	0	(8.2)	(1.007)	(8.6)	22.0	0.270	0.46	0.37

[a] details on seed particles given in Table 1; [b] number-average particle diameter. Average sizes and size dispersities calculated by omitting small secondary particles are given in brackets; [c] dispersity of the particle diameter; [d] coefficient of variation of the particle diameter; [e] specific surface area from BET nitrogen adsorption; [f] cumulative pore volume from BET nitrogen adsorption; [g] molar azide content from elemental nitrogen analysis; [h] calculated ratio of found to expected azide content; [i] sample consisted mainly of agglomerated particles; [j] collapsed particles [k] value calculated by measuring less than 100 particles

Microsphere Characterization

Reference samples (no VBA) and microspheres prepared with VBA were analysed by FT-IR spectroscopy. Spectra conformed to the expected constituent poly(styrene-*co*-divinylbenzene) and poly(styrene-*co*-divinylbenzene-*co*-4-vinylbenzyl azide) copolymers. Spectra featured the characteristic signals of the styrene-*co*-divinylbenzene network at ν = 1492 cm^{-1} (aromatic C=C stretching), 795 cm^{-1} (*para*-substituted benzene C–H bending), and 758 cm^{-1} (mono-substituted benzene C–H bending) and, importantly, spectra also gave qualitative evidence of the successful incorporation of azide functionality into microspheres through a strong signal at 2095 cm^{-1} attributed to the asymmetric azide N=N=N stretching vibration. The intensity of this band varied with the VBA feed ratio, qualitatively demonstrating control over the amount of incorporated azide groups, see Figure 1.

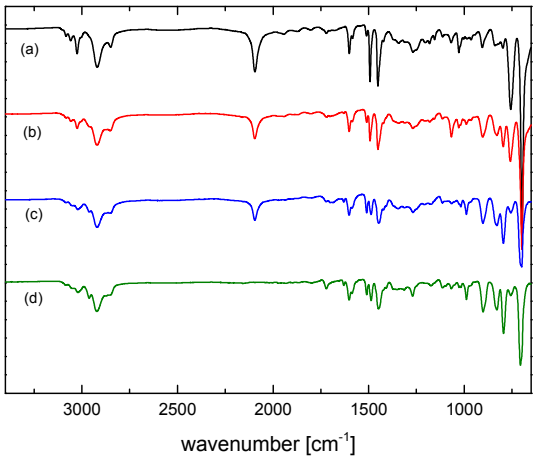

Figure 1: Exemplary FT-IR spectra of microparticles LA4 (a), MA6 (b), HA5 (c) and HA0 (d) showing the characteristic azide stretching band at different intensities at 2095 cm^{-1}

Analysis of samples by SEM revealed uniform spherical microparticles. Average diameters of samples ranged between 7 and 10 µm and did not depend strongly on the DVB:VBA:S feed

ratio. For microparticles with low (< 10 wt%) VBA in the feed, SEM analysis showed very "clean" samples consisting only of uniform spherical particles, which is reflected in very low diameter dispersities, $Đ_d$ < 1.01 and very low coefficients of variation, see Table 2 and Figure 2. As shown in Figure 2, at a constant VBA feed percentage of 5 wt% the relative amounts of DVB and S in the feed govern the surface structure of the particles. While sample LA2 (Figure 2 top; DVB:VBA:S = 16:5:79) showed a clearly bumpy particle surface, the particle surface of sample MA2 (Figure 2, middle; DVB:VBA:S = 50:5:45) was considerably less uneven, and particles from batch HA2 (Figure 2, bottom; DVB:VBA:S = 95:5:0) appeared entirely smooth at the chosen magnification. These results indicated that very well defined uniform microparticles containing (a low amount of) azide functionality with tuneable surface structure could be obtained by substituting styrene with VBA during the seed-swelling polymerization step.

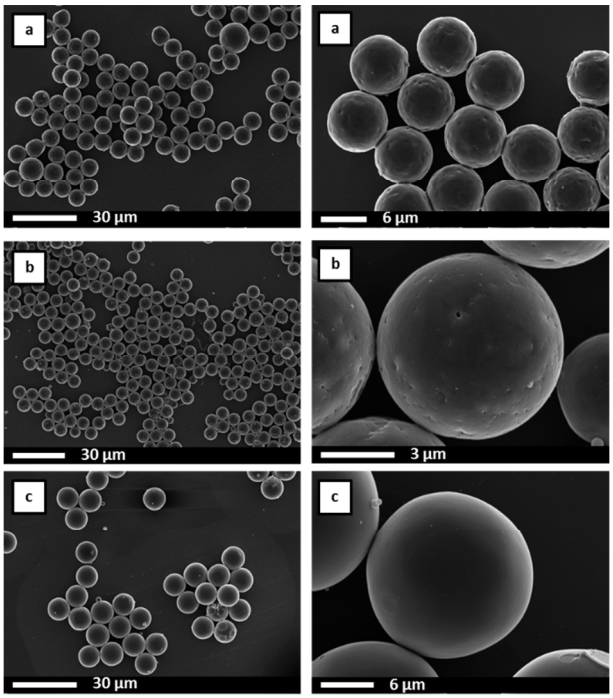

Figure 2. SEM images of microparticles with a low VBA feed amount of 5 wt% and different DVB–S ratios: LA2 (a), MA2 (b), and HA2 (c).

Particle Porosity

Given the influence of the monomer feed ratio on the surface texture, characteristics of the inside structure of microparticles were determined by measuring nitrogen adsorption from which specific surface areas and cumulative pore volumes were calculated using Brunauer-Emmett-Teller (BET) theory. These values, listed in Table 2, allowed for the following observations. Firstly, both parameters, surface area and pore volume, differed dramatically between the three series with values generally increasing with an increasing DVB content. At a constant VBA feed of 10 wt%, for example, sample LA3 (containing 16 wt% DVB) had a specific surface area too small to be quantified by this method, while samples MA4 and HA3 (containing 50, and 90 wt% of DVB, respectively) had measured specific surface areas of 40.2 and 123.2 m^2/g. This observation is in agreement with previous reports[29, 57, 58] and is attributed to a higher rigidity of highly crosslinked copolymers and an earlier phase separation from the seed material during the seed-swelling polymerization which leads to a porous structure. Secondly, measured pore sizes and specific surface areas decreased within each series with an increasing feed ratio of VBA. For the first, low DVB content, series LA this resulted in only the azide-free sample LA0 having a measurable surface area. In series MA samples with 0–10 wt% VBA in feed had measured specific surface areas ranging between 22.1–48.3 m^2/g while samples with higher VBA feed showed lower or no measurable specific surface areas. Specific surface areas and cumulative pore volumes for series HA are plotted in Figure 3. At the highest DVB content of 100% sample HA0 had a measured specific surface area of 341.4 m^2/g and a cumulative pore volume of 0.23 cm^3/g, which reduced drastically with the incorporation of VBA until, above a VBA content of ~ 20%, the specific surface area had reduced to 0. A similar effect of a functional comonomer on the porosity was previously described for the incorporation of vinylbenzyl chloride into porous

microspheres.[22, 23] In case of series HA, the observed drastic decrease of specific surface areas and cumulative pore volumes is not only a result of the increasing VBA concentration. As mentioned above, these value correlate with the amount of DVB crosslinker, which, in case of series HA, is lowered due to substitution with VBA. These results indicate that the incorporation of azide functionality also allows for a tuning of the porosity of the resulting microspheres with observed specific surface areas spanning an impressive range. The high specific surface areas found for series HA suggest the presence of micropores which is in agreement with the smooth surface texture observed by SEM (sample HA2 shown in Figure 2, bottom). SEM images of broken particles providing evidence of the inside structure of particles are shown in the supporting information.

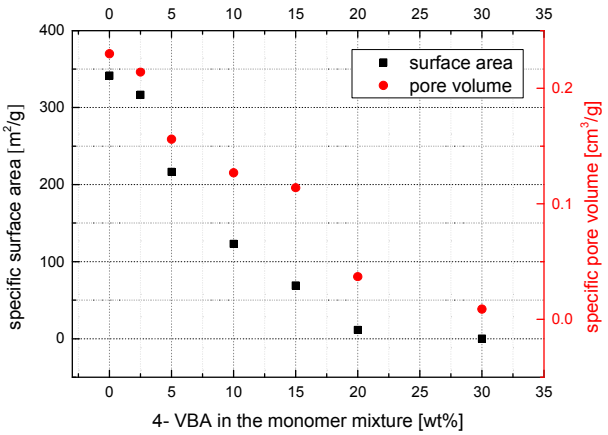

Figure 3: Measured specific surface areas and cumulative pore volumes vs VBA content in the monomer mixture for samples of series HA.

In the context of tuning porosity, it is noteworthy that the molecular weight characteristics of the seed particles have a significant impact on the formation of pores and their structure.[24, 59] While the main objective of the current study is to investigate the feasibility of incorporating (a

large and controllable amount of) of azide functionality into well-defined particles, two experiments with seed particles B (M_w = 44 kg/mol as opposed to 76 kg/mol for seed particles A) are briefly discussed. Samples HB1 and HB2 (Table 2, entries 28 and 29) were prepared with DVB:VBA:S of 95:5:0 and 80:20:0, respectively, and consisted of uniform spherical particles of 8.3 and 7.1 μm diameter, respectively, in good agreement with all three seed A series. While the surfaces of these azide-containing particles (see SEM images in the supporting information) appeared similarly smooth as those of series HA, specific (internal) surface areas and cumulative pore volumes differed strongly, porosimetry yielding significantly higher measured cumulative pore volumes compared to the respective samples with the same feed ratio prepared with seed particles A, i.e. samples HA2 and HA5. SEM of some broken particles of sample HB2 revealed indeed a highly porous inner structure. Interestingly though, sample HB1 had a lower specific surface area than sample HA2 (both with 5 wt% VBA and 95 wt% DVB), suggesting a fundamentally different pore structure between the samples.

VBA Influence on Particle Shape

While the above data shows successful synthesis of well-defined azide-functional microparticles with a low amount of VBA in the monomer mixture, the (albeit slightly) different polarity of VBA compared to S and DVB resulted in several interesting irregularities in formulations with VBA contents above 10 wt-%. For all three series LA, MA, and HA, SEM analysis of samples prepared with more than this amount of VBA in the monomer mixture showed an increasing tendency of microspheres to agglomerate and indicated the formation of smaller particles with diameters of 100 nm–3 μm in addition to the expected microspheres, see Figure 4. Notably, the microspheres as such were generally very uniform, reflected in very low

calculated diameter dispersities and coefficients of variation when the smaller (secondary) particles were omitted in the calculation of these measures of heterogeneity (values calculated by omission of secondary particles are given in parentheses in Table 2).

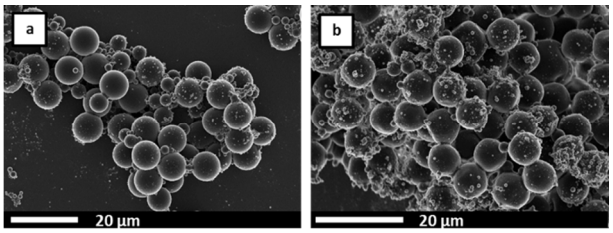

Figure 4. SEM images of (a) sample HA6 (30 wt% VBA) and (b) sample LA7 (25 wt% VBA) showing a large number of smaller particles formed through secondary nucleation in addition to uniform microparticles which are partially fused together (e.g., right image, bottom)

Close observation of the swelling process of seed latexes with monomer mixtures by optical microscopy revealed incomplete swelling with the number of small monomer droplets remaining next to swollen seed particles increasing with the percentage of VBA in feed, see Figure 5. As these remaining monomer droplets increase the overall surface area, the concentration of emulsifier in these formulations may have been too low to stabilise surfaces sufficiently leading to the observed tendency of particles to agglomerate.[25, 56] Incomplete swelling of seeds with monomer mixtures containing VBA was interpreted in terms of a lower miscibility of the more polar VBA with the nonpolar PS seed material, whereas S and DVB showed no limitations in this regard.[52] Additionally, a slightly higher water solubility of VBA compared to S and DVB was considered to contribute to loss of VBA into the water phase and the formation of non-uniform secondary particles through Ostwald ripening.

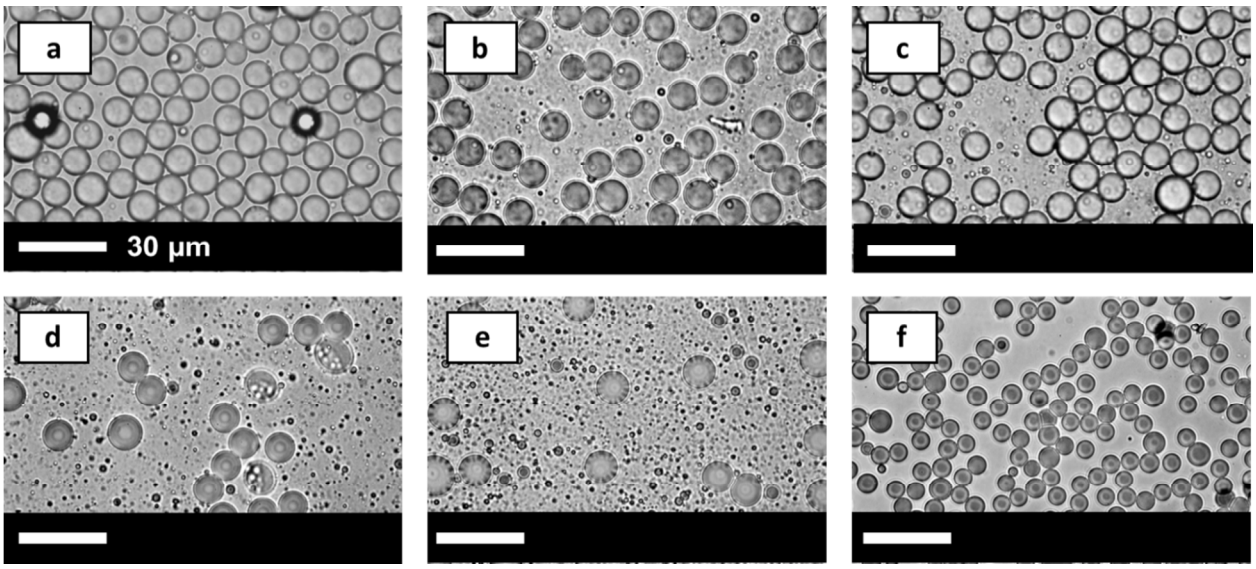

Figure 5: Optical microscopy images recorded during the swelling process of PS seed particles with monomer mixtures containing 50 wt% DVD and different percentages of VBA: (a) 0 wt% VBA showing only swollen seeds; (b) 2.5 wt% VBA; (c) 7.5 wt% VBA; (d) 15 wt% VBA; (e) 30 wt% VBA showing an increasing number of small remaining monomer droplets and (f) DBP-swollen seeds before addition of the monomer mixtures.

For the particle series MA (50% DVB) and HA (only DVB and VBA) dramatic effects on particle shape were observed for formulations with VBA feed ratios of or above 30 wt%. SEM analysis of samples MA8 (DVB:VBA:S = 50:20:30) and MA9 (DVB:VBA:S = 50:30:20) showed dented and partially collapsed particles, see Figure 6A. The observation of several broken particles in an SEM sample of HA7 (DVB:VBA:S = 65:35:0) revealed microspheres to be hollow (Figure 6 BC). This morphology was attributed to an immiscibility of the PS seed particle with the growing crosslinked, azide-functional material resulting in early phase

separation during the polymerization step and the formation of a core–shell structure in which the PS seeds form the core.[21, 60] Upon extraction of the seed material during purification, hollow microspheres are obtained. Volume shrinkage during copolymerization, mechanical stresses during purification, and volume shrinkage upon drying the crosslinked, solvent-expanded, copolymer chains were assumed to impact on the shape of the resulting dried microparticles. Expectedly, particle shells with the highest DVB content proved to be most rigid and dimensionally stable with SEM analysis revealing a large proportion of perfectly spherical, yet hollow, particles for sample HA7. In series MA, on the other hand, the above factors were attributed to cause the observed denting and crushing of the less stable particle shells of samples MA8 and MA9. With an even higher feed percentage of VBA and a presumed earlier and more 'exclusive' separation of PS core and azide-functional shell, sample MA10 (DVB:VBA:S = 50:40:10) was observed by SEM to consist entirely of completely collapsed particles, reminiscent in shape and size of red blood cells, Figure 6D. Interestingly though, the particle diameters (when ignoring dents and imagining collapsed particles re-inflated) and the diameter dispersities (when ignoring small secondary particles) of these samples were similar to all other formulations. This data demonstrates the severe impact of the addition of VBA (despite its very similar chemical structure) and that addition of such a comonomer is a viable and simple means of producing spherical hollow particles.

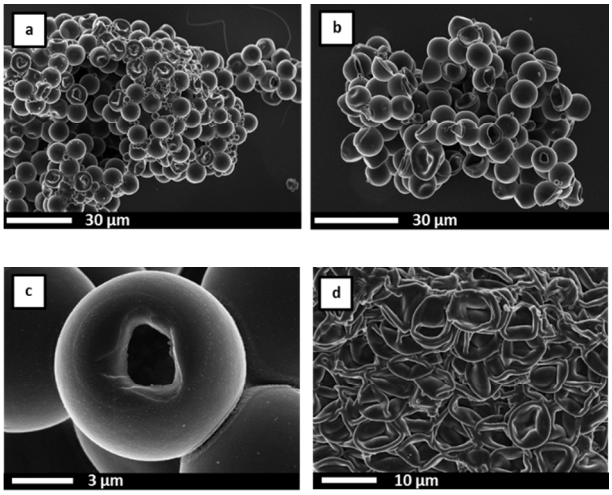

Figure 6: Influence of VBA feed on particle shape: SEM images of (a) dented particles (sample MA8); (b) and (c) hollow spherical particles (sample HA7) and (d) completely collapsed hollow spheres (sample MA10)

Azide Loading

Apart from tuning microsphere morphology including surface area, pore volume, and particle shape as described above, a main motivation for incorporating VBA into microspheres is the high chemical reactivity of the azide functional group and the versatility of associated 'click' chemistries. In order to assess quantitatively the feasibility of incorporating azide functionality into well-defined porous microspheres, all samples were characterised by CHN elemental analysis. The key feature of this analysis was the nitrogen content and results are expressed herein as the ratio of found nitrogen content, N_1, to the calculated nitrogen content expected from the VBA feed ratio, N_0. These values N_0 were calculated for each sample based on the comonomer feed ratios assuming quantitative conversion and take into account the amount of nitrogen introduced by the AIBN initiator (~ 0.2%). This value was experimentally confirmed on

a polystyrene-only sample. Ratios N_1/N_0 were plotted against the VBA feed ratio for the three series LA, MA, and HA, see Figure 7. Notably, this ratio is below unity for all samples, indicating that the found nitrogen content was always below the expected amount. Interestingly though, the data points in Figure 7 suggest a trend that seems particularly obvious for series MA and HA. N_1/N_0 decreases in an apparently linear fashion until a VBA feed ratio of approximately 20 wt% VBA. Above this VBA feed concentration, an apparently constant percentage of approx. 45% of the expected nitrogen is found in the resulting purified particles. For series LA, N_1/N_0 was generally higher with values decreasing likewise with increasing VBA feed.

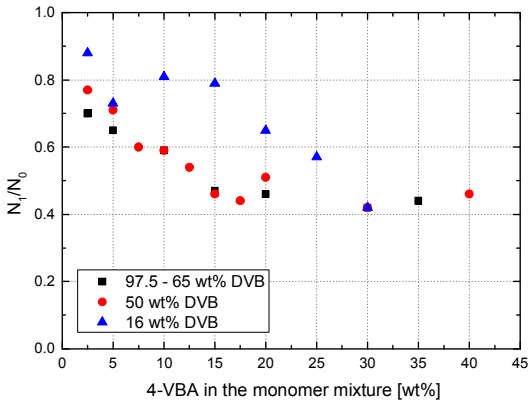

Figure 7: Found/expected nitrogen content ratio N_1/N_0 vs 4-vinylbenzyl azide weight percentage in the in the monomer mixture for the three series LA (triangles), MA (circles), and HA (squares)

These results are in agreement with the notion that VBA did not diffuse quantitatively into the seed particles during the swelling step. Residual VBA-rich monomer droplets, a presumably low concentration of VBA dissolved in the aqueous phase, and predominantly linear polymers formed through auto-initiation within these phases during the polymerization step were expected

to be removed during the purification procedure, thus reducing the amount of found nitrogen and N_1/N_0. Additionally, decomposition and side reactions of the azide functionality during the polymerization step were considered possible factors in reducing N_1/N_0. Loss of azide end group functionality during radical polymerizations[61] and cycloaddition reactions of azides to vinyl groups and subsequent decomposition of the triazoline[62, 63] have been described as common side reactions of azide-functional building blocks during radical polymerizations. In a quantitative study on azide–olefin cycloaddition under radical polymerization conditions, Ladmiral et al., however, demonstrated styrene to be significantly less reactive than acrylic monomers with less than 5% azide loss found after heating to 60 °C for 20 h. In a recent study on linear VBA–S copolymers, we found thermal degradation of the azide functionality (as observed through weight loss by thermogravimetric analysis) only above 230 °C, likewise suggesting general compatibility of the azide functionality with the chosen polymerization conditions.[64] Both factors, incomplete swelling due to polarity difference, and loss to decomposition and/or side reactions, were thus assumed to contribute to the observed loss of nitrogen content.

Two sets of experiments were performed with the aim of improving the swelling behaviour and suppressing the loss of azide functionality. Firstly, since during the swelling step monomers (including VBA) diffuse from droplets into dodecylsulfate-stabilised seed particles, an adverse effect of the negative surface charge on the diffusion of VBA across this layer was considered.[52] In addition to the anionic stabiliser employed for all particles listed in Table 2, seed-swelling polymerizations were carried out using the cationic species dodecyltrimethylammonium bromide (DTAB) and the neutral stabiliser nonylphenol ethoxylate (NPOE) under otherwise unchanged reaction conditions. Results, summarised in the supporting information, however, suggested

little, or no, effect of the stabiliser on the formation of secondary particles at higher VBA feed ratio or the loss of azide functionality as judged from the measured N_1/N_0 ratios.

Secondly, two azide-functional seed particles containing 5 wt-% and 20 wt-% VBA (Table 1, entries C and D), were prepared and used in seed-swelling formulations. It is prudent, at this stage, to reiterate that the linear-chain seed material is removed after particle synthesis. It was, however, presumed that the compatibility between the seed and the monomer mixture would be improved and secondary particle formation suppressed. Notably, this is an ongoing, and apparently promising, approach in our group and detailed results will be published elsewhere. For the sake of the current argument, four samples, HC1, HC2, HD1, HD2 using seeds C and D with either 5 or 20 wt-% of VBA in feed (entries 30–33 in Table 2) are emphasized. Overall, the diameters and diameter dispersities were comparable to microspheres compared from non-functional seeds. Formation of secondary particles for formulations with 20 wt-% VBA was, however, still observed, see Figure 8 and no improvement of particle nitrogen content was observed when comparing the N_1/N_0 ratios of samples HC1, HC2, HD1, HD2 with their counterparts prepared from non-functional seeds with the same VBA–DVB feed ratio, HA2 and HA5. Interestingly though, and clearly visible in the SEM images shown in Figure 8 and data summarised in Table 2, microparticles prepared from the azide-rich seed particles (D) had a highly porous structure with specific pore volumes of 0.49 cm^3/g as measured for sample HC1 and 0.60 cm^3/g for sample HD1. While these two experiments did not bring about an improvement in preventing azide loss during polymerization, the observed drastic impact of using functional seed particles suggests a clear and noteworthy potential of this largely unexplored research avenue in tailoring well-defined porous microspheres.

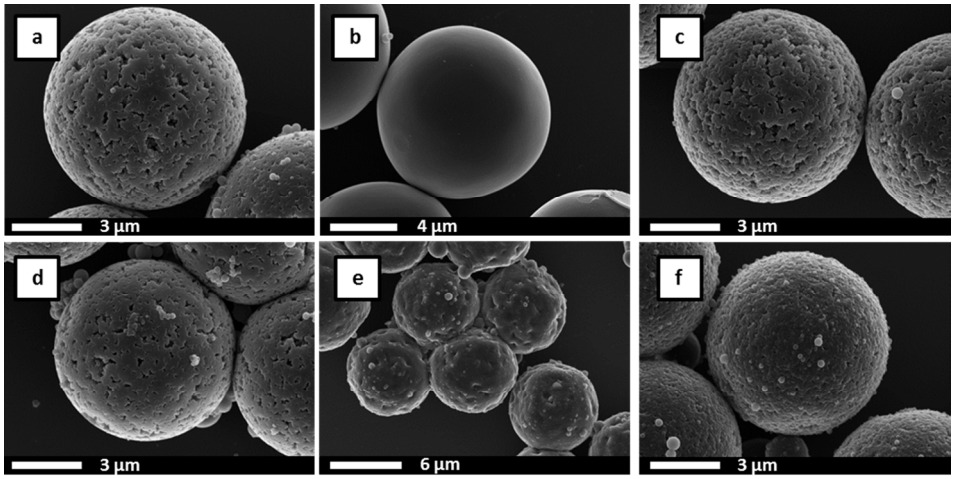

Figure 8: Comparison of microparticles prepared by polymerization of VBA–DVB in seed particles with zero, low, or high VBA content. Upper row: microspheres prepared with 5 wt% 4VBA in monomer mixture and: (a) seeds with low azide concentration (HC1), (b) non-functional seeds (HB1), (c) high concentration of azides in employed seeds (HD1). Bottom row: microspheres prepared with 20 wt% 4-VBA in the monomer mixture and: (d) seeds with low azide concentration (HC2), (e) non-functional seeds (HB2), (f) high azide concentration in employed seeds (HD2).

In spite of the observed loss of azide functionality during the swelling/polymerization step, it is emphasized, that the general concept presented herein—incorporation of VBA comonomer—nevertheless provided control over the final content of highly reactive and chemically versatile azide groups. A plot of calculated azide loading, expressed in mmol/g, versus VBA feed ratio for series MA and HA, shown in Figure 9, indicated a near-linear trend with good agreement between the two series and tuneable azide loadings spanning a range from 0.1–1.2 mmol/g. Markedly, this maximum azide content is higher than the maximum azide concentration we

achieved in a previous study where residual vinyl groups in P(S–DVB) microspheres where chemically transformed in two steps into 1-azidoethyl substituents.[29]

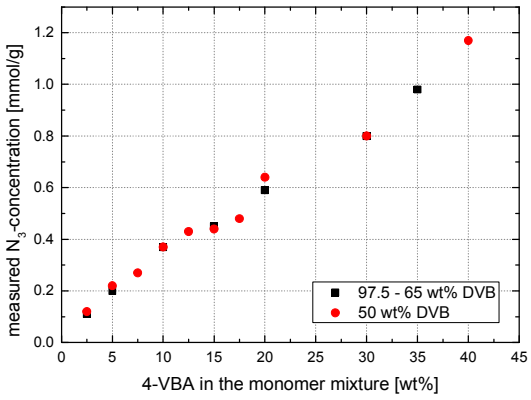

Figure 9: Azide concentration vs VBA feed in the monomer mixture for series MA (circles) and HA (squares)

Microsphere Functionalization

With a series of porous, azide-functional microparticles in hand, the chemical accessibility of the azide groups was next demonstrated through azide–alkyne cycloaddition modifications. In addition to the commercially available phenylacetylene, an alkyne-functional Rhodamine B reagent (prepared through esterification of the Rhodamine B acid functionality with propargyl alcohol) was employed as a fluorescent label. A selection of microspheres including samples LA7, MA9, HA6, featuring different DVB feed ratios but comparable azide loadings of approx. 0.8 mmol/g were modified with both alkynes (supplied in threefold excess with regards to azide groups) under inert atmosphere in the presence of catalyst CuBr, ligand tetramethylethylenediamine, auxiliary base triethylamine, and solvent DMF. Modified particles were purified by exhaustive washing procedures until no evidence of remaining reagents (colour in case of the dye alkyne) in the washings was detectable.

Conversions, listed in Table 3, were determined by IR-spectroscopy based on the disappearance of the strong azide N=N=N absorbance at 2095 cm^{-1} through integration of this signal after standard normal variate corrections of spectra, Figure 10. For the sample with the lowest crosslinking density, LA7, quantitative conversion was observed with phenylacetylene and the Rhodamine B alkyne. For the more densely crosslinked substrates MA9 and HA6, conversions were incomplete, but above 50% in all cases. Unsurprisingly, conversions were higher, up to 73%, with the less sterically challenged phenylacetylene. Overall, these values are in good agreement with literature conversions.[29]

Table 3. Summary of CuAAC Click Modification Reactions on Microparticles

Substrate	Azide Loading[a] (mmol/g)	Azide Conversion[b] (%)	
		phenylacetylene	Rhodamine B alkyne
LA7	0.78	100	100
MA9	0.80	73	52
HA6	0.80	84	56

[a] calculated from CHN analysis; [b] determined by IR spectroscopy

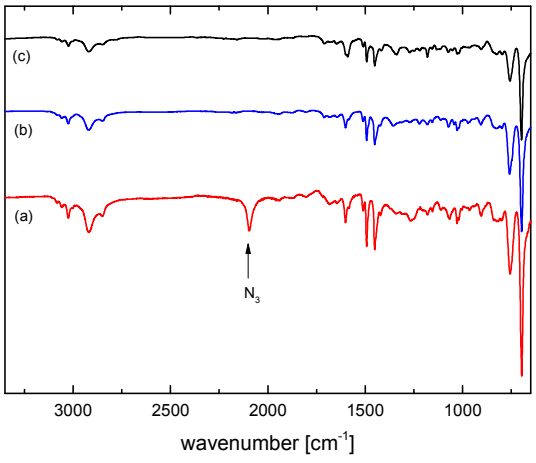

Figure 10. FT-IR spectra of azide-functional microspheres LA7 (a), after azide-alkyne cycloaddition with phenylacetylene (b), and after clicking with Rhodamine B alkyne (c) indicating complete disappearance of the azide vibrational band

In addition to visual characterization (Rhodamine B labelled microspheres presented as intensely purple powder), this fluorescent label allowed for analysis through confocal laser scanning fluorescence microscopy. A fluorescence cross section taken through the equator of a single particle, shown in Figure 11, indicated a much higher dye concentration, and thus click labelling efficiency, in the outer layer of the particle. This was presumed to reflect both a higher VBA concentration in the particle corona due to phase separation during the swollen seed polymerization as discussed above, as well as a higher accessibility of VBA units to the bulky dye in the outer particle layer. Notably, however, click modification occurred throughout the entire thickness of the particle with significant fluorescence detected in the particle cores. Together, this data demonstrates successful modification of azide-functional porous particles.

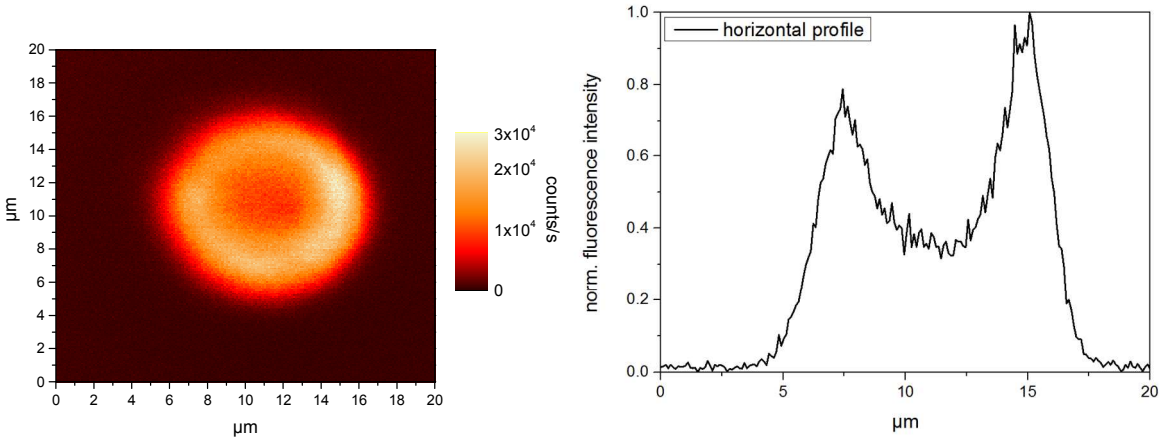

Figure 11. Confocal laser scanning fluorescence cross sectional image of a single MA09 particle after modification with Rhodamine B alkyne and normalised fluorescence intensity profile.

Conclusions

Seed-swelling polymerization formulations provide simple access to microparticles of tuneable size and porosity. However, this procedure is optimized for poly(styrene-*co*-divinylbenzene) and the incorporation of functional groups typically requires elaborate yet inefficient post-synthesis modification steps. Herein, the feasibility of including 4-vinylbenzyl azide (VBA), as a prototypical 'clickable' monomer, in seed-swelling copolymerizations is investigated for the first time in detail. The synthesis of azide-functional particles with high azide loadings of up to 1.17 mmol/g was successful. However, the inherent polarity difference of VBA and VBA-containing copolymers compared to styrene and the resulting immiscibility with the polystyrene seed material revealed both challenges and opportunities of this synthetic approach. Incomplete swelling of seed particles with VBA is discussed as a main reason for the formation of small, secondary particles and for lower-than-expected azide content of resulting particles. The use of azide-functional seed particles is proposed as a method to reduce incompatibility. On the other side, the incorporation of VBA also provided a versatile handle to tune particle porosity and, exploiting phase separation between seed particle and growing VBA-rich copolymer, offered an elegant approach to produce hollow crosslinked, spherical, reactive microparticles. Modification of azide groups with functional alkynes was possible throughout the thickness of microparticles with confocal fluorescence microscopy of Rhodamine B alkyne click-modified particles revealing a higher concentration of (accessible) azide functionality in the corona of the particles, in agreement with early phase separation inside seed particles. As a very detailed study, this work addresses key difficulties in exploiting seed-swelling polymerization formulations for the preparation of reactive microparticles. Offering control over particle porosity, shape, and

functional group density, this approach is expected to advance fundamental and applied research in this growing field.

Acknowledgements.

The authors thank Renate Walter (Zoological Institute, University of Hamburg) for SEM image measurements. Tim Hadler at the Institute for Physical Chemistry is acknowledged for confocal scanning fluorescence microscopy measurements. P.J.R. acknowledges the Australian Research Council (ARC) for past funding through a Discovery Early Career Researcher Award (DE120101547). M.A., W.P., and H.-U.M. acknowledge the German Federal Ministry of Education and Research (BMBF) for financial support (13N11312).

References

1. M. R. Buchmeiser, *Journal of Chromatography A*, 2001, **918**, 233-266.
2. F. M. B. Coutinho, M. A. F. S. Neves and M. L. Dias, *Journal of Applied Polymer Science*, 1997, **65**, 1257-1262.
3. S. Punna, E. Kaltgrad and M. G. Finn, *Bioconjug Chem*, 2005, **16**, 1536-1541.
4. E. Unsal, S. T. Camli, S. Senel and A. Tuncel, *Journal of Applied Polymer Science*, 2004, **92**, 607-618.
5. K. F. Bolton, A. J. Canty, J. A. Deverell, R. M. Guijt, E. F. Hilder, T. Rodemann and J. A. Smith, *Tetrahedron Letters*, 2006, **47**, 9321-9324.
6. A. Kirschning, H. Monenschein and R. Wittenberg, *Angewandte Chemie*, 2001, **113**, 670-701.
7. J. H. Schutten, C. H. Van Hastenberg, P. Piet and A. L. German, *Die Angewandte Makromolekulare Chemie*, 1980, **89**, 201-219.
8. H. Kawaguchi, *Progress in Polymer Science*, 2000, **25**, 1171-1210.
9. M. T. Gokmen and F. E. Du Prez, *Progress in Polymer Science*, 2012, **37**, 365-405.
10. C.-W. Chen and C.-Y. Chen, *Colloid and Polymer Science*, 2009, **287**, 1377-1389.
11. D. Cochin, A. Laschewsky and F. Nallet, *Macromolecules*, 1997, **30**, 2278-2287.
12. P. J. Dowding, J. W. Goodwin and B. Vincent, *Colloids and Surfaces A: Physicochemical and Engineering Aspects*, 1998, **145**, 263-270.
13. S. E. Shim, S. Yang, M.-J. Jin, Y. H. Chang and S. Choe, *Colloid and Polymer Science*, 2004, **283**, 41-48.
14. R. A. Prasath, M. T. Gokmen, P. Espeel and F. E. Du Prez, *Polymer Chemistry*, 2010, **1**, 685.
15. S. Xu, Z. Nie, M. Seo, P. Lewis, E. Kumacheva, H. A. Stone, P. Garstecki, D. B. Weibel, I. Gitlin and G. M. Whitesides, *Angew Chem Int Ed Engl*, 2005, **44**, 724-728.
16. J. Ugelstad, A. Berge, T. Ellingsen, O. Aune, L. Kilaas, T. N. Nilsen, R. Schmid, P. Stenstad, S. Funderud, G. Kvalheim, K. Nustad, T. Lea, F. Vartdal and H. Danielsen, *Makromolekulare Chemie. Macromolecular Symposia*, 1988, **17**, 177-211.
17. J. Ugelstad, K. H. Kaggerud, F. K. Hansen and A. Berge, *Die Makromolekulare Chemie*, 1979, **180**, 737-744.
18. J. Ugelstad, H. R. Mfutakamba, P. C. Mørk, T. Ellingsen, A. Berge, R. Schmid, L. Holm, A. Jørgedal, F. K. Hansen and K. Nustad, *Journal of Polymer Science: Polymer Symposia*, 1985, **72**, 225-240.
19. J. Ugelstad, P. C. Mórk, K. H. Kaggerud, T. Ellingsen and A. Berge, *Advances in Colloid and Interface Science*, 1980, **13**, 101-140.
20. B. Thomson, A. Rudin and G. Lajoie, *Journal of Applied Polymer Science*, 1996, **59**, 2009-2028.
21. S. Baruch-Sharon and S. Margel, *Colloid and Polymer Science*, 2009, **287**, 859-869.
22. J.-W. Kim, J.-G. Park, J.-H. Ryu, I.-S. Chang and K.-D. Suh, *Colloid and Polymer Science*, 2005, **283**, 1233-1240.
23. Y.-C. Liang, F. Svec and J. M. J. Fréchet, *Journal of Polymer Science Part A: Polymer Chemistry*, 1997, **35**, 2631-2643.
24. J.-W. Kim and K.-D. Suh, *Journal of Industrial and Engineering Chemistry*, 2008, **14**, 1-9.

25. C. M. Cheng, F. J. Micale, J. W. Vanderhoff and M. S. El-Aasser, *Journal of Polymer Science Part A: Polymer Chemistry*, 1992, **30**, 235-244.
26. C. M. Cheng, J. W. Vanderhoff and M. S. El-Aasser, *Journal of Polymer Science Part A: Polymer Chemistry*, 1992, **30**, 245-256.
27. M. Omer-Mizrahi and S. Margel, *Journal of Polymer Science Part A: Polymer Chemistry*, 2007, **45**, 4612-4622.
28. Q. C. Wang, F. Švec and J. M. J. Fréchet, *Journal of Polymer Science Part A: Polymer Chemistry*, 1994, **32**, 2577-2588.
29. M. Albuszis, P. J. Roth, W. Pauer and H.-U. Moritz, *Polymer Chemistry*, 2014, **5**, 5689-5699.
30. B. Karagoz, Y. Y. Durmaz, B. N. Gacal, N. Bicak and Y. Yagci, *Designed Monomers & Polymers*, 2009, **12**, 511-522.
31. K. L. Hubbard, J. A. Finch and G. D. Darling, *Reactive and Functional Polymers*, 1999, **39**, 207-225.
32. K. L. Hubbard, J. A. Finch and G. D. Darling, *Reactive and Functional Polymers*, 1999, **42**, 279-289.
33. B. R. Stranix, J. P. Gao, R. Barghi, J. Salha and G. D. Darling, *The Journal of Organic Chemistry*, 1997, **62**, 8987-8993.
34. A. S. Goldmann, A. Walther, L. Nebhani, R. Joso, D. Ernst, K. Loos, C. Barner-Kowollik, L. Barner and A. H. E. Müller, *Macromolecules*, 2009, **42**, 3707-3714.
35. G. Bayramoglu, B. Karagoz, B. Altintas, M. Y. Arica and N. Bicak, *Bioprocess Biosyst Eng*, 2011, **34**, 735-746.
36. M. Bacquet, C. Caze, J. Laureyns and C. Bremard, *Reactive Polymers, Ion Exchangers, Sorbents*, 1988, **9**, 147-153.
37. A. R. Mitchell, S. B. H. Kent, M. Engelhard and R. B. Merrifield, *The Journal of Organic Chemistry*, 1978, **43**, 2845-2852.
38. D. R. Breed, R. Thibault, F. Xie, Q. Wang, C. J. Hawker and D. J. Pine, *Langmuir*, 2009, **25**, 4370-4376.
39. M. Kedem and S. Margel, *Journal of Polymer Science Part A: Polymer Chemistry*, 2002, **40**, 1342-1352.
40. C. N. Urbani, C. A. Bell, D. E. Lonsdale, M. R. Whittaker and M. J. Monteiro, *Macromolecules*, 2007, **40**, 7056-7059.
41. W. H. Binder and R. Sachsenhofer, *Macromolecular Rapid Communications*, 2008, **29**, 952-981.
42. W. H. Binder and R. Sachsenhofer, *Macromolecular Rapid Communications*, 2007, **28**, 15-54.
43. K. Kempe, A. Krieg, C. R. Becer and U. S. Schubert, *Chem Soc Rev*, 2012, **41**, 176-191.
44. J. E. Moses and A. D. Moorhouse, *Chem Soc Rev*, 2007, **36**, 1249-1262.
45. V. V. Rostovtsev, L. G. Green, V. V. Fokin and K. B. Sharpless, *Angewandte Chemie International Edition*, 2002, **41**, 2596-2599.
46. B. S. Sumerlin and A. P. Vogt, *Macromolecules*, 2010, **43**, 1-13.
47. M. T. Gokmen, W. Van Camp, P. J. Colver, S. A. F. Bon and F. E. Du Prez, *Macromolecules*, 2009, **42**, 9289-9294.
48. A. K. Oyelere, P. C. Chen, L. P. Yao and N. Boguslavsky, *The Journal of Organic Chemistry*, 2006, **71**, 9791-9796.
49. C. E. Evans and P. A. Lovell, *Chem Commun (Camb)*, 2009, 2305-2307.

50. M. Slater, M. Snauko, F. Svec and J. M. J. Fréchet, *Analytical Chemistry*, 2006, **78**, 4969-4975.
51. Ç. Kip, B. Maraş, O. Evirgen and A. Tuncel, *Colloid and Polymer Science*, 2013, **292**, 219-228.
52. K. Ouadahi, E. Allard, B. Oberleitner and C. Larpent, *Journal of Polymer Science Part A: Polymer Chemistry*, 2012, **50**, 314-328.
53. V. Rodionov, H. Gao, S. Scroggins, D. A. Unruh, A.-J. Avestro and J. M. J. Fréchet, *Journal of the American Chemical Society*, 2010, **132**, 2570-2572.
54. W. Yang, W. Ming, J. Hu, X. Lu and S. Fu, *Colloid and Polymer Science*, 1998, **276**, 655-661.
55. T. Bahar and A. Tuncel, *Polymer Engineering & Science*, 1999, **39**, 1849-1855.
56. Q. Zhang, Y. Han, W. Wang, T. Song and J. Chang, *J Colloid Interface Sci*, 2010, **342**, 62-67.
57. Q. Liu, Y. Li, S. Shen, Q. Xiao, L. Chen, B. Liao, B. Ou and Y. Ding, *Journal of Applied Polymer Science*, 2011, **121**, 654-659.
58. J. Wei, X. Tang, X. Wang and J. Yan, *Journal of Applied Polymer Science*, 2005, **96**, 2071-2078.
59. A. Srisopa, A. M. Imroz Ali and A. G. Mayes, *Journal of Polymer Science Part A: Polymer Chemistry*, 2011, **49**, 2070-2080.
60. M. Okubo and H. Minami, *Colloid and Polymer Science*, 1997, **275**, 992-997.
61. G. Mantovani, V. Ladmiral, L. Tao and D. M. Haddleton, *Chemical Communications*, 2005, 2089-2091.
62. G. T. Anderson, J. R. Henry and S. M. Weinreb, *The Journal of Organic Chemistry*, 1991, **56**, 6946-6948.
63. Y. Li, J. Yang and B. C. Benicewicz, *Journal of Polymer Science Part A: Polymer Chemistry*, 2007, **45**, 4300-4308.
64. M. Albuszis, P. J. Roth, W. Pauer and H.-U. Moritz, *in preparation*.

Table of Contents use only

Synthesis and in-depth characterization of reactive, uniform, crosslinked microparticles based on free radical copolymerization of 4-vinylbenzyl azide

Marco Albuszis, Peter J. Roth, Franziska Exnowitz, Doris Locsin Wong, Werner Pauer, and Hans-Ulrich Moritz

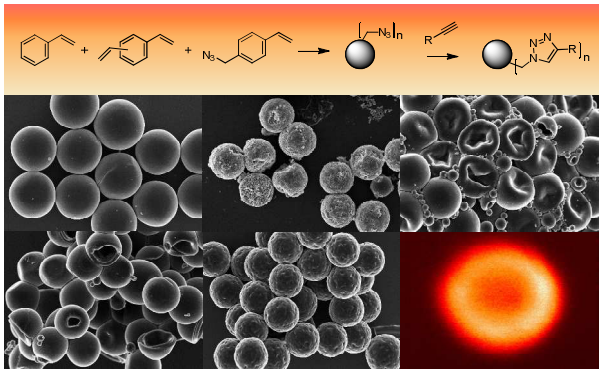

A direct seed-swelling copolymerization formulation affords well-defined azide-functional porous or hollow microparticles amenable to click-modification.